

# DESIGN ANALYSIS OF ROLLING CONTACT BEARINGS

<sup>1</sup>M.Amareswari Reddy, <sup>2</sup>T.Hima Bindu, <sup>3</sup>M.N.V.Krishna Veni, <sup>4</sup>D.Srinivasa Rao

<sup>1,4</sup> Phd Scholar, Department of mechanical Engineering, Andhra University,  
<sup>2,3</sup> Assistant Professor, <sup>2</sup>Raghu Engineering College, <sup>3</sup>ANITS Engineering College.

**Abstract :** A bearing is a machine part whose function is to support another moving machine element. It is also used to guide the motion of the element while preventing motion in the direction of applied load. Bearing takes up the radial and axial loads imposed on the moving element they carry and transmit these to the machine frame. Rolling-element bearings consist of balls or rollers positioned between raceways that conform to the shape of the rolling element. Depending on the bearing design, the loads acting on the bearing may be radial or axial loads. These loads may leads to elastic deformation at the contact between the rolling elements and the raceways. The aim of this work is to analyze the pressure distribution acting at the contact area and various stresses on the rolling elements by considering bearing parameters such as curvature and roller.

The design and the analysis of bearing are carried out using Mechanical Desktop and ANSYS Work Bench respectively. The result of this study reveals that as the curvature and diameter of the roller has profound influence on the pressure and frictional stress acting at the contact area. Hence, the curvature and diameter of the roller are important parameters for effective design of any bearing. Apart from the above bearing parameters number of rollers of the bearing also have signification role in minimizing the pressure and frictional stress at the contact area.

**Keywords -** Roller bearing, radial and axial loads, contact area, Mechanical Desktop, Ansys work bench.

## I. INTRODUCTION

A bearing is a machine part designed to reduce friction between moving parts or to support moving loads. A machine part, whose function is to, supports another moving machine element. It is also used to guide the motion of the element while preventing motion in the direction of applied load and transmit these loads to the machine frame. There are two main kinds of bearings: the journal bearing and the antifriction type. The anti-friction bearing, such as the roller bearing and the ball bearing, operating on the principle of rolling friction. The bearing consists of Outer Ring, Inner Ring, Balls or Rollers. Rolling Bearings consist of two circular steel rings as shown in fig. 1. One of the rings is much larger than the other. This larger ring is referred to as the Outer Ring. The smaller ring is referred to as the Inner Ring.

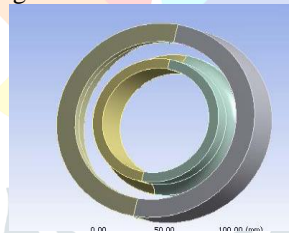


Fig 1 Inner and Outer Ring Model

A bearing consists of a set of rolling elements, which are known as Balls or Rollers. A predetermined number of solid balls or rollers are formed into geometric shapes and placed at equal intervals in the open space between the two rings. The load applied on the bearings is transmitted through the rolling elements from Outer Ring and Inner Ring vice versa. The rolling elements are classified according to their as geometric shapes as shown in fig.2



Fig. 2 Types of Rolling Elements

## II. LITERATURE REVIEW

Dowson et.al. [1] Provides a comprehensive presentation of the history of bearings such as a ball and roller bearings. The general use of rolling bearings did not occur until the Industrial Revolution. Ret i [2] et.al., however, showed that balls have universal motion while rollers can move in one direction alone. But if balls or rollers touch each other in their motion, they will make the movement more difficult than if there was no contact between them, because their touching is by contrary motions and this friction causes contrariwise movements. In this regard Tallian et.al. [3] extended that the modern rolling bearing consists of three eras that is empiric al era, classical era and the modern era. The author Weibull, W., A tistical [4] had consider only the applied loading when bearing operating speeds are nominal. The rolling element loading under this condition, which might also be termed static loading. Jones, A et.al. [7] had taken clearance into the consideration and derived an equation for max contact pressure for a roller bearings having zero internal radial clearance and subjected to a simple radial load. Chiu, Y. et.al. [9] had considered two

bodies of revolution having different radii of curvature in a pair of principal planes passing through the contact between the bodies may contact each other at a single point under the condition of no applied load. Harris, T[22] had extended the study to evaluate the contact area between the inner race and the roller for the cylindrical roller bearings. Peng Chunjun[10] had reached on the static analysis of an angular contact ball bearing using Finite Element Method. By considering the important influencing parameters for radial stiffness of the bearing under an axial load. By taking ball bearing with the radius of ball around 22 mm and the inner and outer groove radii around 11mm. The author had evaluated the reaction forces on the bearing. Patrick Tibbitts [11] have studied the deflection of the support structure of a tapered roller thrust bearing load along the roller-to-raceway contact. The race and roller have tighter curvatures, the contact stress increases and bearing life decreases. By modifying the support structure, reduces contact stress and increases life.

From the above discussion it is clear that still there is so much to study on the bearings by considering different parameters. It is necessary to improve the existing mathematical models to understand the stress and the pressure at the contact area of the bearing. In this work it is intended to develop a Bearing to study the effects of pressure and the stress at the contact area of the bearing. By considering the bearing parameters such as curvature, diameter of the roller. The model was developed in Mechanical Desktop and analysis is carried out in ANSYS to evaluate the best result.

**III. ANALYTICAL SOLUTION**

The analytical solution of the rolling bearing elements can be carried in different models for finding the stress and contact pressure at the bearing contact area. For cylindrical roller bearing an Infinitesimal Line Loading of an Elastic Half Space method is carried out for solving the maximum contact pressure. For tapered bearing Hertz contact theory is carried out for finding maximum stress and pressure for the bearing when it is in contact.

**3.1 Line loading of an elastic half space**

The simplest semi-infinite geometry is the case of a planar semi-infinite (infinite in one axis) solid body loaded in the normal direction along a line on the surface. The x-y plane defines the surface, the loading line is along the y-axis, and the load is along the z direction. Figure shows the axis and dimension definitions

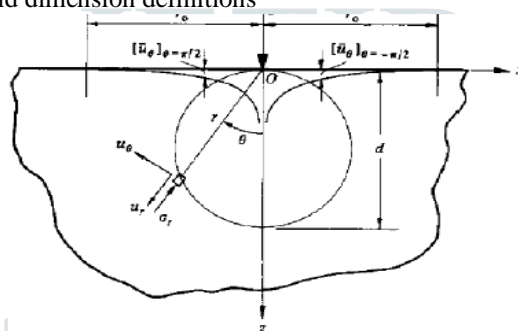


Fig. 3 Line Loading of an Elastic Half-Space

The solution in the polar space is:

$$\phi(r, \theta) = A r \theta \sin \theta$$

From the equations of elasticity, the three components of stress is given as:

$$\sigma_r = \frac{1}{r} \frac{\partial \phi}{\partial r} + \frac{1}{r^2} \frac{\partial^2 \phi}{\partial \theta^2}, \sigma_\theta = \frac{\partial^2 \phi}{\partial r^2} \text{ and } \tau_{r\theta} = -\frac{\partial}{\partial r} \left( \frac{1}{r} \frac{\partial \phi}{\partial \theta} \right)$$

Therefore,  $\sigma_\theta = \tau_{r\theta} = 0$

So that the stresses are entirely radial from the line of contact  $\sigma_r = \frac{2A \cos \theta}{r}$

**3.2 Parallel cylinders in contact**

Considering two cylinders of arbitrary radii with parallel axes, contacting each other under no load, so that the contact area is simply a line. The x-axis is placed tangent to both cylinders and normal to the axes of the cylinders. The y-axis is parallel to the cylinder axes, along the line of contact. The z-axis will then be along a line running through the centers of the cylinders circular cross sections.

By considering the following assumptions, the surface profile of the each cylinder may be represented as:

$$z_i = A_i x^2 + B_i y^2 + C_i xy + D_i x^3 \dots, \text{ where } i = 1, 2, \text{ for each cylinder}$$

The unloaded separation distance between the two points at the same x-coordinate on the two cylinders

$$h = z_1 - z_2$$

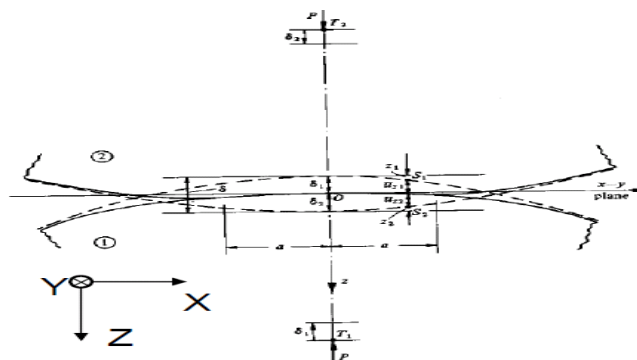


Fig.4 Contacting Parallel Cylinders

Where  $z_1$  and  $z_2$  can be expressed in terms of the radii of curvature of the solid in the principal axes.

$$R' = \left( \frac{1}{R_1} + \frac{1}{R_2} \right)^{-1} \text{ Such that } h = \frac{1}{2R'} x^2 = \frac{1}{2} \left( \frac{1}{R_1} + \frac{1}{R_2} \right) x^2$$

Hence this relation gives the separation between surface contours in the undeformed and unloaded state.

**2.3 Theoretical Analysis for Stress calculations**

The contact zone between the roller-end and rib creates an ellipsoidal surface compressive stress distribution, is shown in Fig. 5

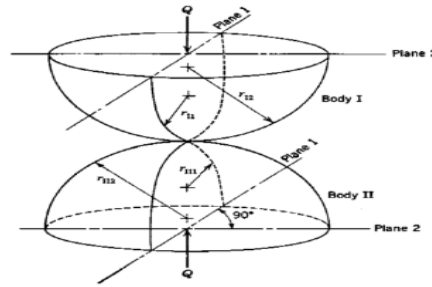


Fig. 5 Point Contact

The roller end has a spherical radius, and the rib face is flat at an angle  $\alpha$ . The maximum compressive Hertzian contact stress is

given as:  $\sigma_{max} = \frac{3Q}{2\pi ab}$

**3.4 Pressure Calculations**

For the roller body- raceway contacts under ideal line contact the following equations are used

$$P_{max} = \frac{2Q_{i,o}}{\pi l_{eff} b_{i,o}}$$

**3.5 Analytical Model Results**

For illustrative purposes, a specific set of dimensions and properties has been chosen as shown in Table 1&2, to facilitate comparison between the mathematical and computer analyses. These parameters are typical of bearings in use in modern industry.

Table 1: Material Properties

Material Specification	AMS6490 Bearing Steel
Elastic Modulus (E)	100,000 MPa
Poisson's ratio (v)	0.29 (dimensionless)

Table 2: Bearing Geometric Properties

Normal Load P	100N
Bearing roller radius R1	10mm
Bearing race radius R2	infinite

**3.5.1 For Cylindrical Roller Bearing**

Inserting the example dimensions into the equations derived in above section provides the following values:

$$R' = \left( \frac{1}{R_1} + \frac{1}{R_2} \right)^{-1} = \left( \frac{1}{10\text{mm}} + \frac{1}{\infty} \right)^{-1} = 10\text{mm} \tag{E.1}$$

$$E^* = \left( \frac{1-v_1^2}{E_1} + \frac{1-v_2^2}{E_2} \right)^{-1} = \left( 2 \cdot \frac{1-0.29^2}{100,000\text{MPa}} \right)^{-1} = 54,591\text{MPa} \tag{E.2}$$

$$a = 2 \sqrt{\frac{P \cdot R'}{\pi \cdot E^*}} = 2 \sqrt{\frac{100\text{N} \cdot 10\text{mm}}{\pi \cdot 54,591\text{MPa}}} = 0.153\text{mm} \tag{E.3}$$

$$P_{max} = \left( \frac{P E^*}{\pi R'} \right)^{1/2} = \left( \frac{100\text{N} \cdot 54,591\text{MPa}}{\pi \cdot 10\text{mm}} \right)^{1/2} = 417\text{MPa} \tag{E.4}$$

**3.5.2 For Tapered Roller Bearing**

Inserting the example dimensions into the equations derived in above section provides the following values:

$$Q_o = \frac{\text{Applied Thrust}}{z \sin(\alpha_o)} = \frac{35,000}{17 \sin(18)} = 29650\text{N}$$

$$\omega_c = \frac{1}{2} \left( 1 - \left( \frac{D_{mean}}{d_m} \right) \cos(\alpha_{dm}) \right) \omega_i = \frac{1}{2} \left( 1 - \left( \frac{1.425}{9.7} \right) \cos(15.75) \right) 8000 = 3434.4 \text{ RPM}$$

$$F_c = \frac{1}{8} \rho \pi D_{mean}^2 l_t d_m \omega_c^2 = \frac{1}{8} (0.3) \pi (1.425)^2 (1.9) (9.7) (3434.4)^2 = 6227 \text{ N}$$

$$Q_f = \frac{Q_o \cos(\alpha_o) - F_c - \frac{Q_o \sin(\alpha_o)}{\tan(\alpha_i)}}{\left( -\cos(\alpha_f) - \frac{\sin(\alpha_f)}{\tan(\alpha_i)} \right)} = \frac{6662.5 \cos(18) - 1399.3 - \frac{6662.5 \sin(18)}{\tan(13.5)}}{-\cos(13.5) - \frac{\sin(13.5)}{\tan(13.5)}} = 3780 N$$

$$p_{max} = \frac{2Q_{i.o}}{\pi d_{eff} b_{i.o}} = \frac{2(6662.5)}{\pi(1.9)(0.01483)} = 103 MPa$$

**IV. 2D FEM ANALYSIS ON THE BEARING**

The purpose of the finite element analysis was to determine the various stresses between roller and the inner ring and maximum contact area . The stresses on the surface and below the surface of the inner ring were investigated. ANSYS Workbench software package was used for the finite element simulation. This package provided 2D and 3D modeling .The finite element solutions were in compliance with maximum load capacity.

The model is imported from Mechanical Desktop to ANSYS Workbench, then the meshing is automatically generated for model. “Mesh sizing” can be used in order to generate a reasonable or better mesh. Fig.6 shows the mesh generated model of the bearings, the elements for the roller are tetrahedral and the inner ring and outer ring are hexahedron elements.

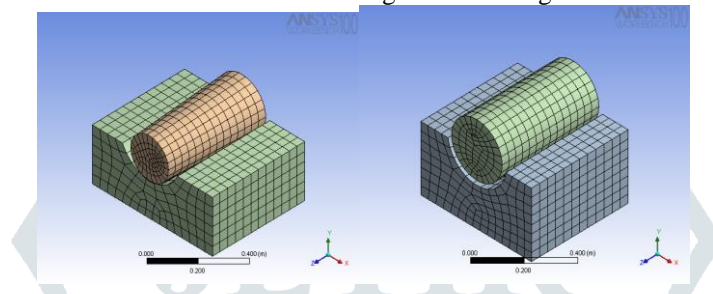


Fig. 6 Mesh Generated on Cylindrical and Tapered Bearing

Fig.7 shows the materials for the inner, outer ring and roller are linear isotropic structure steel. Young’s modulus and Poisson’s ratio for design and analysis of bearing is as shown below

Structural Steel	
<b>Structural</b> Add/Remove Properties	
<input type="checkbox"/> Young's Modulus	2.e+011 Pa
<input type="checkbox"/> Poisson's Ratio	0.3
<input type="checkbox"/> Density	7850. kg/m³
<input type="checkbox"/> Thermal Expansion	1.2e-005 1/°C
<input type="checkbox"/> Alternating Stress	
<input type="checkbox"/> Strain-Life Parameters	
<input type="checkbox"/> Tensile Yield Strength	2.5e+008 Pa
<input type="checkbox"/> Compressive Yield Strength	2.5e+008 Pa
<input type="checkbox"/> Tensile Ultimate Strength	4.6e+008 Pa
<input type="checkbox"/> Compressive Ultimate Strength	0. Pa
<b>Thermal</b> Add/Remove Properties	
<input type="checkbox"/> Thermal Conductivity	60.5 W/m·°C
<input type="checkbox"/> Specific Heat	434. J/kg·°C
<b>Electromagnetics</b> Add/Remove Properties	
<input type="checkbox"/> Relative Permeability	10000
<input type="checkbox"/> Resistivity	1.7e-007 Ohm·m

Fig. 7 Material Overviews

Analysis setting deals with the load to be applied to the structure, including load steps, load magnitude and load direction. For one static structure analysis, there can be one or several load steps. For each load step, several sub steps can be set in order to make the solution converge better and result more accurate. Fig. 8 shows one of the bearing model analysis settings. There are totally 10 steps and for the first step there are initially 10 sub steps and it has maximum 100 sub steps.

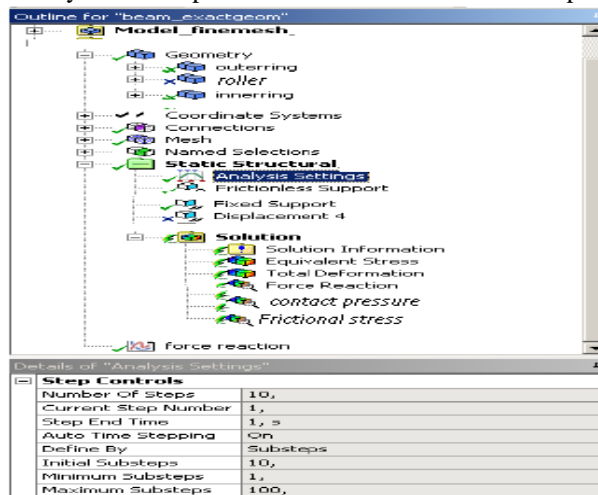


Fig.8 Analysis Setting

The lower surface of the Outer ring is constrained in all DOF. A 100N force is applied downward on the roller for this model. When the solution is done, the stresses, contact pressure, contact status, and max contact pressure etc. on the bearing are evaluated.

As the curvature and diameter of roller is varying the pressure distributed on roller increases at the contact area. This is because as radius of roller is greater than the curvature, the contact area between them is reduced as result the stress at the contact area is increased. Fig 9 shows the pressuredistribution on the roller.

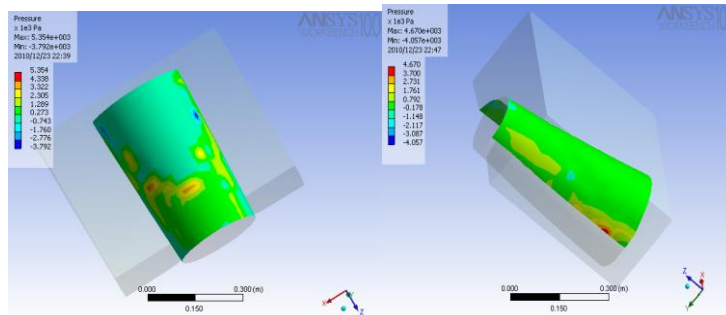


Fig. 9 Pressure Distribution on the Rollers

Fig10 shows the equivalent stress distribution on the roller, by changing the curvature and the diameter of roller there is a variation in friction stress. As the diameter of roller changes the stress on the roller increases.

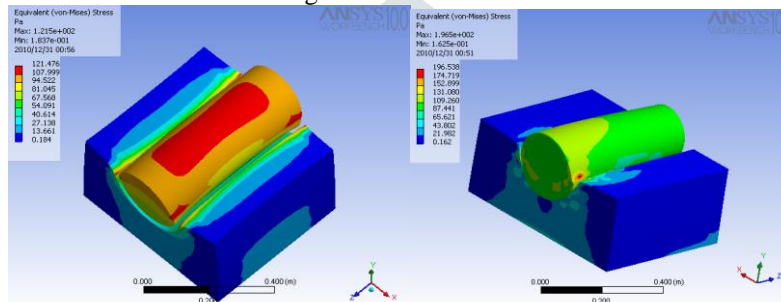


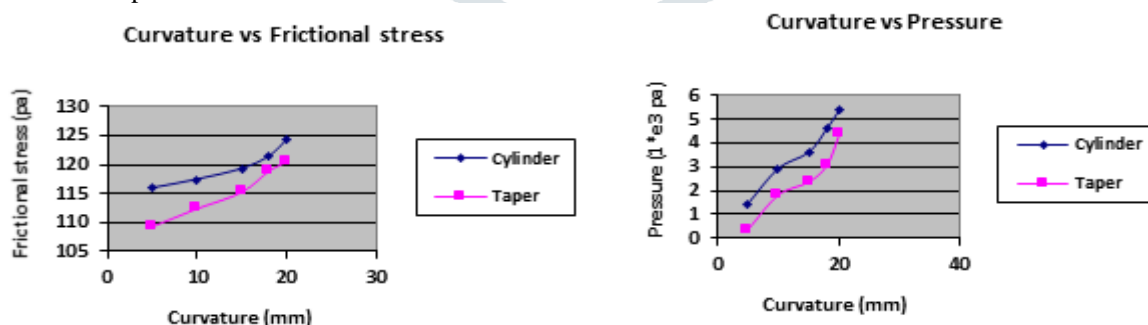
Fig. 10 Equivalent Stress Distribution on the Rollers

A 100N force is applied downward on the cylindrical and tapered rollers of different curvature is tabularized for 18mm diameter rollers as shown in the table 3.

Curvature(mm)	Frictional stress (pa)		Pressure (1*e3pa)	
	Cylindrical	Tapered	Cylindrical	Tapered
5	115.9	109.39	1.39	0.34
10	117.43	112.43	2.92	1.81
15	119.32	115.22	3.62	2.36
18	121.476	118.76	4.65	3.07
20	124.37	120.37	5.43	4.36

Table3: 18mm diameter roller

The graph for frictional stress and pressure distributions for a 18mm diameter roller is plotted is shown in graph 1. As the curvature increases the pressure and the frictional stress also increases.



Graph1: Frictional stress and pressure distributions for a 18mm diameter roller

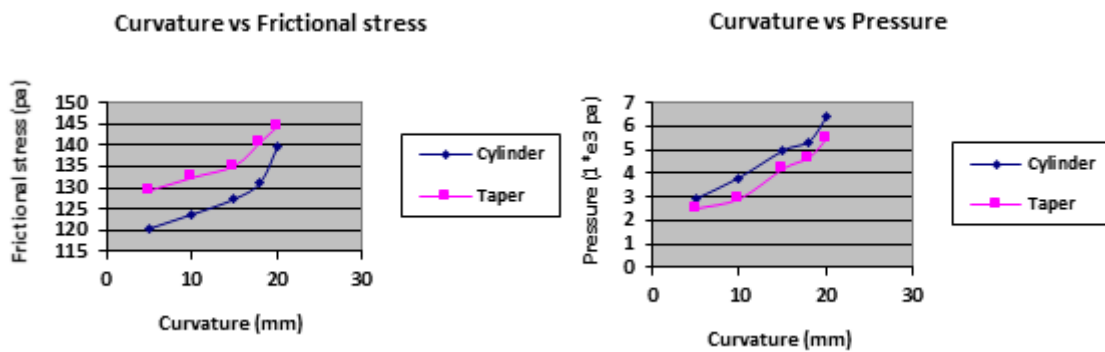
A 100N force is applied downward on the cylindrical and tapered rollers of different curvature is tabularized for 20mm diameter rollers as shown in the table 4

Curvature(mm)	Frictional stress (pa)		pressure (1*e3pa)	
	Cylindrical	Tapered	Cylindrical	Tapered
5	120.32	129.39	2.91	2.54
10	123.69	132.43	3.82	2.96
15	127.35	135.22	4.96	4.21
18	131.25	140.76	5.35	4.67
0020	139.65	144.37	6.41	5.96

Table 4: 20mm diameter roller



The graph for frictional stress and pressure distributions for a 20mm diameter roller is plotted is shown in graph 1. As the curvature increases the pressure and the frictional stress also increases.



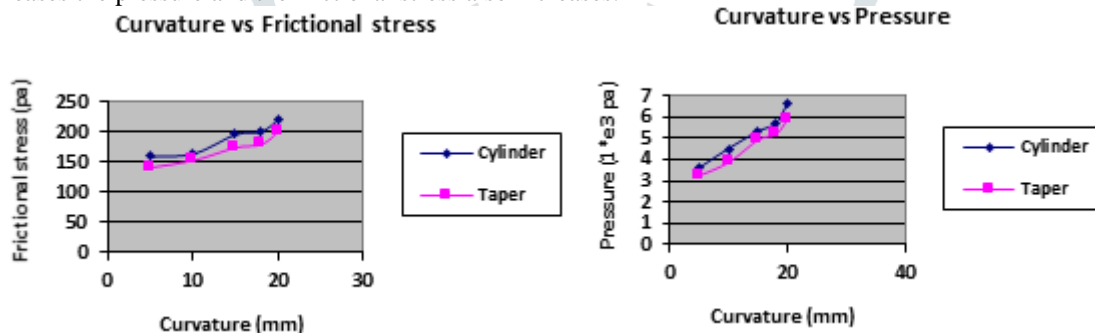
Graph2: Frictional stress and pressure distributions for a 20mm diameter roller

A 100N force is applied downward on the cylindrical and tapered rollers of different curvature is tabularized for 22mm diameter rollers as shown in the table 5

Curvature(mm)	Frictional stress (pa)		Pressure (1*e3pa)	
	Cylindrical	Tapered	Cylindrical	Tapered
5	160.89	141.53	3.61	3.23
10	165.25	153.37	4.52	3.87
15	196.35	175.34	5.32	4.96
18	200.91	180.54	5.69	5.22
20	220.36	202.23	6.62	5.94

Table 5; 22mm diameter roller

The graph for frictional stress and pressure distributions for a 22mm diameter roller is plotted is shown in graph 1. As the curvature increases the pressure and the frictional stress also increases.



Graph3: Frictional stress and pressure distributions for a 22mm diameter roller

From above tabulated values, the best value of curvature is taken, as 20mm for the roller diameter of 18mm, as the frictional stress and pressure distributions at the contact area is more flexible than compared to other values.

Considering the best value of curvature and radius of roller which was obtained in 2-D analysis, Using Mechanical Desktop a 3-D roller bearing is designed and analysis is carried out by increasing the number of rollers. The distance between each roller must be as minimum as possible as so that the bearing can have a more life time as number of rollers increases the pressure and the stress distributed on the rollers is evenly distributed and their values are decreased as a result that the bearing can use for a long time without failure. More over at some extension overlapping of rollers takes place which result in failure of bearing.

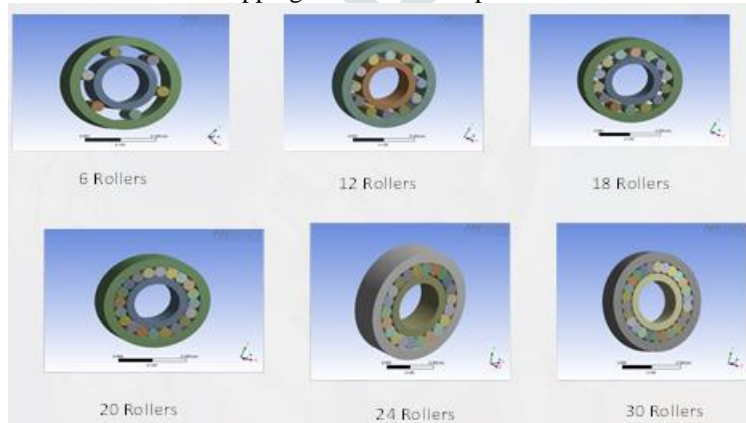


Fig. 11: Increasing Number of Rollers

As the number of roller is increasing the pressure distributed on roller decreases at the contact area. This is because as number of roller is increases the load evenly distributed on the rollers which result to decreases in pressure. Fig. 12 shows the Pressure distribution on cylindrical and tapered Bearing consists of 8 cylindrical rollers and 13 tapered rollers.

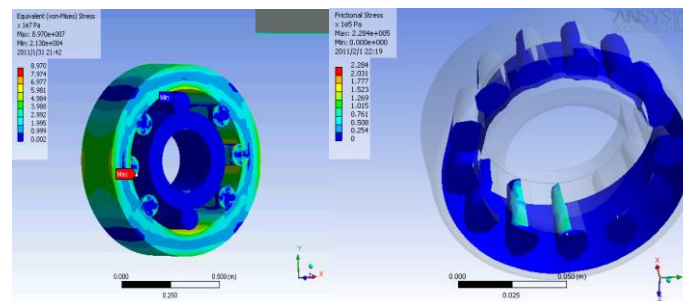


Fig. 12: Pressure Distribution on Cylindrical and Tapered Bearing

The frictional stress and von misses stress of 100N force is applied downward on the cylindrical and tapered rollers is tabularized for different number of rollers, is shown in the table 6

No. of rollers	Frictional stress( $1 \times 10^5$ pa)		Von misses stress( $1 \times 10^7$ pa)	
	Cylindrical	Tapered	Cylindrical	Tapered
6	2.52	1.79	8.97	7.01
8	2.89	1.93	7.91	5.92
13	3.42	2.28	6.09	4.86
18	3.64	2.59	5.25	3.49
24	4.58	3.25	4.69	3.02
30	4.76	3.75	3.96	2.22

Table 6: Frictional stress and von misses stress for different number of rollers.

For the cylindrical roller and tapered roller bearing, the rollers from 13 to 18 can be used. Beyond that, if the roller number is increased the failure occurs in bearing due to the increase of weight of the bearing.

## V. CONCLUSION

Based on the detailed literature review, it has been observed that several methodologies have been adopted for analyzing the pressures distribution and stress acting at the contact area of the bearing. Based on the literature, initially analytical calculation was done for the tapered roller bearing and cylindrical roller bearing for estimation of above mentioned output parameters. The analysis is carried out by taking into consideration of different parameters that influencing the bearing failure.

It is difficult to calculate all the theoretical values for the each parameter that influence the design of the bearing. Hence, these have been estimated by using Ansys software package. Based on the obtained results the following Conclusions can be drawn

1. As the curvature varies the pressure and frictional stress varies at the contact area. Similarly as the diameter of the roller varies, variation is observed in pressure and frictional stress at the contact area.
2. Hence the curvature and diameter of roller are important parameters for analysis of the pressure and stresses at the contact area therefore leading for better design of the bearing.
3. As the curvature is varying the pressure acting at the contact area of the tapered roller bearing is decreasing by 6.75% than that of cylindrical roller bearing. Similarly the frictional stress distributed at the contact area of the tapered roller bearing is decreasing by 14.56% than that of cylindrical roller bearing.
4. The stresses and the pressure of the roller decreases by increasing the number of rollers, more over at some extension overlapping of rollers takes place which result in failure of bearing.
5. The von misses stress of the tapered roller bearing is differing by 16.4% than that of cylindrical roller bearing. Whereas frictional stress of the tapered roller bearing is differing by 8.67% than that of cylindrical roller bearing. By increasing the number of rollers in tapered and cylindrical roller bearing.

From the obtained results it can be concluded that out of the cylindrical and tapered roller bearing, taper bearing is better suitable than that of cylindrical roller bearing since whenever the loading is combination of radial and axial.

## VI. ACKNOWLEDGMENT

I would like to express my deep sense of gratitude and indebtedness to Dr. K.N.S. Suman, Associate Professor, Department of Mechanical Engineering, Andhra University College of Engineering, Visakhapatnam for his inspiring guidance, valuable suggestions and constant encouragement throughout my thesis work. I owe him lots of gratitude for having me shown my way of work. I extend my sincere thanks to non-teaching staff working in the computer lab for their co-operation. With due regards I acknowledge the inspiration and blessings of my parents and my friends, who encouraged and provided the necessary support for the completion of this work.

## VII. REFERENCE

1. Dowson, D., History of Tribology, 2nd ed., Longman, New York, 1999.
2. Reti, L., Leonardo on bearings and gears, Scientific American, 224(2), 101–110, 1971.
3. Tallian, T., Progress in rolling contact technology, SKF Report AL690007, 1969.
4. Hamrock, B., Jacobson, B., and Schmid, S., Fundamentals of Machine Elements, McGraw-Hill, New York, 1999.
5. Zaretsky, E.V.: STLE Life Factors for Rolling Bearings. STLE SP-34, Society of Tribologists and Lubrication Engineers, Park Ridge, IL, 1992.
6. Lundberg, G.; and Palmgren, A.: Dynamic Capacity of Rolling Bearings. Acta Polytech., Mechanical Engineering Series, vol. 1, no. 3, 1947
7. Jones, A.B.: Analysis of Stresses and Deflections. General Motors Corporation, Bristol, CT, 1946.
8. From Contact Mechanics, Johnson, K.L., United Kingdom, 1985

9. Chen J Q, Zhou H, Xu L L. Review of theoretical research on the load distribution in roller bearing [J]. Journal of Beijing Institute of Petro-chemical Technology, 2000, 8(1) : 47-52. (in Chinese)
10. Peng Chunjun “Static Analysis of Rolling Bearings Using Finite Element Method” may 2009
11. ‘Tapered Roller Thrust Bearing and Support Structure ‘ by Patrick Tibbits Emerson Power Transmission
12. Analysis of subsurface crack propagation under rolling contact loading in railroad wheels using FEM Yongming Liu, Liming Liu, Sankaran Mahadevan Vanderbilt University, Nashville, TN 37235, USA
13. Contact Stress Concentration due to Surface Irregularity in Cylindrical Rolling Element Bearings by Jeffrey A. Scarcella Rensselaer Polytechnic Institute Hartford, CT December, 2008
14. Tallian, T. and Gustafsson, O., Progress in rolling bearing vibration research and control, ASLE Paper 64C-27, October 1964.
15. Scanlan, R., Noise in rolling-element bearings, ASME Paper 65-WA/MD-6, November 1965.
16. Sayles, R. and Poon, S., Surface topography and rolling element vibration, in Precision Engineering, IPC Business Press, 1981
17. Gustafson, O. et al., Final report on the study of vibration characteristics of bearings, U.S. Navy Contract Nobs-78552, U.S. Navy Index No. NE 071 200, December 6, 1963.
18. DenHartog, J., Mechanical Vibrations, 4th ed., McGraw-Hill, New York, 1956
19. Vince Adams and Abraham Askenazi; Bilding Btter Products with Finite Element Analysis; on world press,1998
20. T.Stolarski Y.Nakasone. S.Yoshimoto; Engineering analysis with ANSYS software; Elsevier Butterworth-Heinemann, Oxford, 2006
21. Weibull, W., A tatistical representation of fatigue failure in solids, Acta Polytech. Mech. Eng., Ser. 1, No. 9, 49, Royal Swedish Acad. Eng., 1949.
22. T.A. Harris, Rolling Bearing Analysis, Fourth Edition, John Wiley and Sons, New York (2001).
23. S. Timoshenko and J. Goodier, Theory of Elasticity, 3<sup>rd</sup> ed., McGraw-Hill, New York (1970).
24. Cornish, Robert F.; Orvos, Peter S.; and Gupta, Shionarayan R.: Development of High Speed Tapered Roller Bearing. IR-1, Timken Roller Bearing Co., 1973. (AFAPL-TR-73-85, AD-771547).
25. Conners, T. F.; and Morrison, F. R.: Feasibility of Tapered Roller Bearings for Main-Shaft Engine Applications. SKF Industries, Inc Report AL73T009, 1973 (USAAMRDL-TR-73-46).
26. W.Wang, P.L. Wong, and Z. Zhang: Partial EHL analysis of rib-roller contact in tapered roller bearings. Tribology International Vol. 29, No. 4, pp. 313-321, 1996.
27. D. Brewe and B. Hamrock, “Simplified Solutions for Elliptical – Contact Defor-mations Between Two Elastic Solids”, ASME Trans., J. Lub. Tech. 101 (2), 231-239 (1977).
28. [http://www.kmlbearing.cn/common/catalog\\_data/01/0101/010101/01010101/ image\\_01010101\\_b.gif](http://www.kmlbearing.cn/common/catalog_data/01/0101/010101/01010101/ image_01010101_b.gif)
29. <http://www.promshop.info/cataloguespdf/a005-011.pdf>.
30. Release 11.0 Documentation for ANSYS.